

# The synthesis and binding properties of nano-scale hydrophobic pockets

Corinne L. D. Gibb, Huaping Xi, Peter A. Politzer, Monica Concha and Bruce C. Gibb\*

*Department of Chemistry, University of New Orleans, New Orleans, LA 70148, USA*

Received 25 May 2001; revised 8 August 2001; accepted 9 August 2001

**Abstract**—Computational investigations into the conformational preferences of previously reported host **4** are presented. Single point calculations, in conjunction with NMR evidence, indicate that the open conformation is considerably more stable than the closed form. The thermodynamic binding parameters for nano-scale host **4** encapsulating a range of halogenated guests are reported. Association constants for guests as small as bromobenzene, to as large as 3[(1*R*)-endo]-(+)-bromocamphor, were determined in both deuterated chloroform and toluene-*d*<sub>8</sub>. The unavailability of large guests prevented determining the optimal guest to cavity volume ratio for this rigid host. In contrast however examining a range of small guests indicated that in the less competitive toluene, binding only occurred with guests that filled greater than 33% of the cavity. As anticipated all halogenated guests were noted to bind halogen atom down, indicating that the formation of C–H···X–R hydrogen bonds is a major contributor to complex stability. Three related hosts with more open cavities were synthesized to evaluate the effects of preorganization of the cavity walls on guest binding. Binding studies with the best guest for **4**, 1-iodoadamantane, demonstrated that cavity wall integrity and rigidity is essential for strong binding. These results are set in context of how de Novo active-site syntheses may provide access to new catalysts with tailored properties and/or substrate selectivities. Important considerations relating to this task, and possible ways in which the field may develop in accomplishing this goal, are also briefly discussed. © 2002 Elsevier Science Ltd. All rights reserved.

## 1. Introduction

In the most general of terms, there are two ways by which we can be inspired to develop new catalysts. Either we can be inspired by nature, or we can be motivated by chemical syntheses devised in the laboratory. Evolution has seen to it that nature's enzymes epitomize near perfect chemical synthesis—for a broad range of molecular conversions. Consequently enzymes provide a particularly strong motivation for scientists interested in developing highly efficient, and environmentally friendly, chemical processes. Interestingly, these different sources of inspiration have often resulted in the effective separation of the fields of enzyme mimicry and wholly non-natural, catalyst development. However en mass<sup>1</sup> these approaches are beginning to show what we can and cannot do to form atom economical,<sup>2</sup> efficient catalysts.

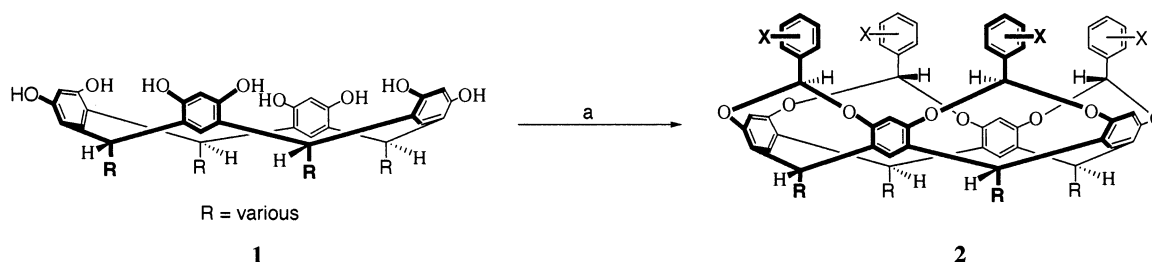
The long-term goal of our research is primarily concerned with the design of catalysts that utilize synthetic molecular cavities for selective substrate transformation. However, before we can begin to address catalysis by de Novo active-site design, we need to consider the problem of synthesizing hydrophobic cavities that will recognize the desired substrates and (ultimately) incorporate the necessary

catalytic machinery for chemical conversion. To be able to form significant non-covalent interactions with a sizable substrate (>10 non-hydrogen atoms) the cavity must both be sufficiently encapsulating, i.e. concave, and of nanometer dimensions. However, along with cavity size, the cavity shape (symmetry) and the cavity portal size must also be factored into the design if the desired physicochemical properties are to be obtained. Furthermore, interwoven with all these subtleties must be a synthetic strategy that will engender a molecular architecture incapable of undergoing collapse. An enzyme uses  $\alpha$ -helices,  $\beta$ -sheets and  $\beta$ -turns, and the rest of the protein matrix to prevent collapse of its hydrophobic pocket. A synthetic cavity that is atom economical cannot rely on such 'luxuries.'

Access routes to relatively small rigid cavities have been well established for some time now, with the calixarenes,<sup>3,4</sup> resorcinarenes,<sup>5</sup> and cyclotrimeratrylenes<sup>6</sup> serving as common starting points. However designing converging binding sites capable of binding a molecule or moiety comprised of say ten or more non-hydrogen atoms has proven difficult. Consequently there have been relatively few reports concerning the development of large molecular cavities of an integral<sup>7–10</sup> or dynamic nature.<sup>11–16</sup> We describe here our latest investigations into the binding properties of nano-scale molecular basket **4**<sup>7</sup> (Scheme 2). As we shall demonstrate, one particularly interesting feature of this host is its structural rigidity. Thus, it shows strong binding for guests that are reasonably comparable in size to

*Keywords:* cavitand; host–guest chemistry.

\* Corresponding author. Tel.: +1-504-280-6311; fax: +1-504-280-6860; e-mail: bgibb@uno.edu



**Scheme 1.** (a) benzal bromide,  $K_2CO_3$  or DBU.

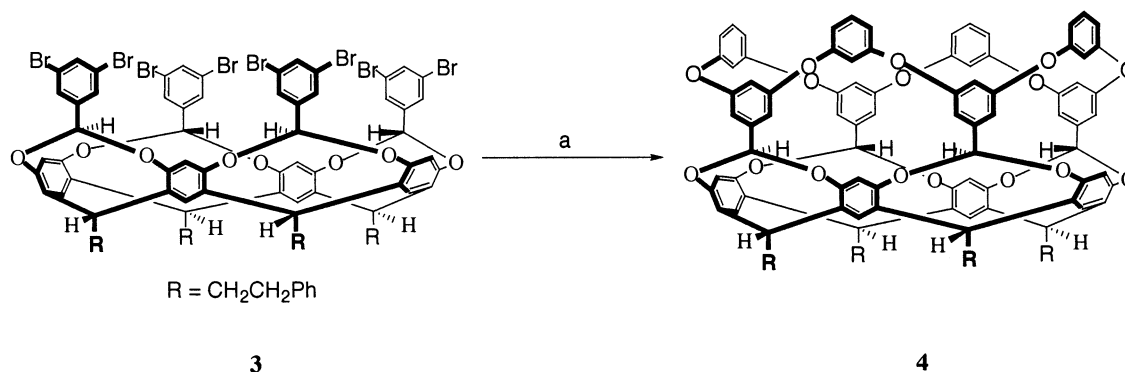
the cavity, but much weaker binding for small guests that must reside in a ‘partial vacuum’ when bound in the cavity. We also detail the synthesis and binding properties of a series of related hosts with cavities which, although of the same size as **4**, are more open and prone to collapse. Finally, we take the opportunity to gaze into a crystal ball and suggest some possible avenues that molecular cavity design will take in the next few years.

## 2. Discussion and results

The stereoselective bridging of resorcinarenes, such as **1**, with benzal bromides (Scheme 1) has figured prominently in our recent research efforts. The resulting deep-cavity cavitands (DCCs), e.g. **2**, offer their cavities to a number of aspects of supramolecular chemistry.<sup>17–19</sup> Although their synthesis involves the irreversible formation of eight covalent bonds and the generation of four stereogenic centers, yields of these compounds as high as 65% have been observed. Consequently access to multi-gram quantities of bowl-shaped DCCs possessing a variety of functional groups is possible. We have investigated the binding proper-

ties of a number of DCC derivatives similar to **2** ( $R = CH_2CH_2Ph$ ), as well as related ‘dimers’,<sup>20</sup> but have observed nothing but perhaps the weakest of interactions with potential guests. We attribute this observation to the fact that each of the second row aromatic rings is free to rotate around its benzal carbon/*ipso* carbon bond. Following this hypothesis we embarked on a study to investigate ways in which we could efficiently link the second row of aromatic rings together. Conceptually it seemed most appropriate to do this while at the same time extending the size of the molecular cavity further. Thus we used octabromide **3** to synthesize basket molecule **4** (Scheme 2).<sup>7</sup> The eight aryl-aryl ether bonds are each formed with an efficiency of >98%, which results in host **4** being isolated in a very satisfying 88% yield.

The  $^1H$  NMR of basket **4** is indicative of a compound with  $C_{4v}$  symmetry. However two possible  $C_{4v}$  isomers, which barring their ‘roofs’ have remarkably similar shaped cavities, can arise from this Ullmann reaction. Either the third row of aromatic rings can be directed inwards towards the  $C_4$  axis of the molecule, or they can be directed outwards (Fig. 1). There are therefore two possibilities to consider. It



**Scheme 2.** (a) resorcinol,  $K_2CO_3$ , CuO.

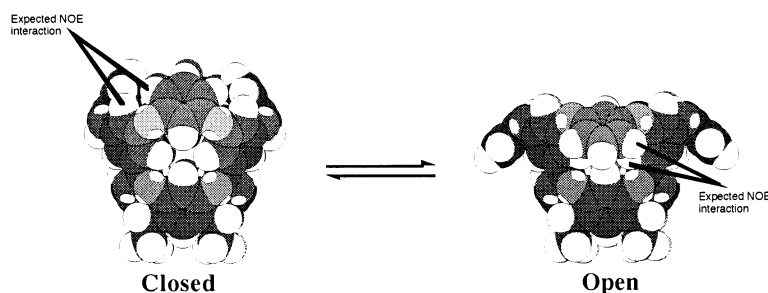


**Figure 1.** The two  $C_{4v}$  conformers of host **4**. Signature NOEs are indicated.

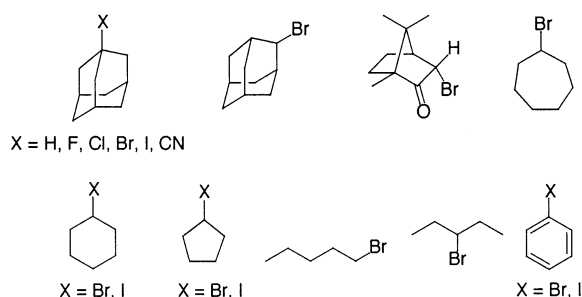


**Figure 2.** Guests examined for their affinity to basket **4**.

is conceivable that as depicted in Fig. 1, an equilibrium exists between the open and closed conformers of **4**. Alternatively it may be the case that the barrier to this conformational flipping is too large, and that even at the elevated reaction temperatures no equilibrium exists and only one isomer is kinetically favored during synthesis. In other words the reaction is highly diastereoselective. The previously determined X-ray structure of **4** complexed with 1-iodoadamantane<sup>7</sup> reduced these options somewhat by showing the host to possess an open conformation. In other words this form would appear to be either the kinetic product of reaction or, at least in the solid phase, the more thermodynamically stable one. It may also of course be both. To investigate this situation we first turned to NOESY <sup>1</sup>H NMR studies as models suggested that both the open and the closed forms of **4** should possess signature interactions (Fig. 1). Using CD<sub>2</sub>Cl<sub>2</sub> as solvent we observed cross-peaks consistent with the open conformation. In contrast no cross-peaks were observed that would indicate the presence of the closed conformer. Thus if an equilibrium between the two structures is present, it is heavily in favor of the open form. Whether or not an equilibrium between the open and closed host exists could not be determined by variable temperature <sup>1</sup>H NMR. Thus an examination of CD<sub>2</sub>Cl<sub>2</sub> solutions of **4** down to  $-90^{\circ}\text{C}$  failed to show any signal splitting indicative of a conformational flipping process slowing down to the NMR time-scale.<sup>21</sup> Likewise, the establishment of an equilibrium process could not be observed in a <sup>1</sup>H NMR VT experiment up to  $100^{\circ}\text{C}$  (toluene-*d*<sub>8</sub>).

To complement the NMR results we turned to computational approaches. First, to conform the stability of the two conformers we took the structure determined by crystallography, and a model of the closed conformer built and minimized using MM2,<sup>22</sup> and optimized both using the Gaussian 98 system at the STO-3G level.<sup>23</sup> The resulting structures differed in overall energy by  $19\text{ kcal mol}^{-1}$  in favor of the open conformation. We subsequently took the analysis one step further and carried out single point calculations to obtain total energies with the density functional SVWN procedure using the 6-31G\* basis set.<sup>24</sup> Again the open conformation was noted to be the most stable, but this time by a considerable  $\Delta E=40\text{ kcal mol}^{-1}$ . It is not yet clear why there is such a difference in energy between the two structures. However undoubtedly contributing to the stabilization of the open conformation is the presence of twelve C–H... $\pi$  interactions between the four aromatic rings of the third row and the underlying protons from both the first and second rows of rings (those partially

obscured in the right-hand structure of Fig. 1). As for the question of the possible equilibrium between the two conformers, we used AM1 to perform structural minimizations of the host, as the dihedral angles defining the relationship between one (flipping) resorcinol type ring and the cavity were changed. We began with the higher energy closed conformation and changed the dihedral angles pertaining to one ring in  $12^{\circ}$  increments, calculating the overall energy of each structure. These investigations indicated that the energy barrier for the forward process ( $\Delta G_{\text{for}}^{\ddagger}$ , for the flip from the higher energy conformation when all rings are closed, to the lower energy conformer where one is in the open position) is somewhere in the region of  $3\text{ kcal mol}^{-1}$ , while the reverse process ( $\Delta G_{\text{rev}}^{\ddagger}$ ) is somewhere in the region of  $7\text{ kcal mol}^{-1}$ . Thus we did not observe any changes in the NMR of **4** down to  $-90^{\circ}\text{C}$  because: (1) so little of the closed form actually exists in solution and; (2) the energy barrier for flipping one ring is quite small.

Considering the size and shape of the cavity of basket **4** we envisioned substituted adamantanes to be ideal guests.<sup>25</sup> We have expanded on our initial examination of adamantanes binding to **4**,<sup>7</sup> and present in Table 1 the collective association constants for a number of different guests (Fig. 2) in both CDCl<sub>3</sub> and toluene-*d*<sub>8</sub>. To investigate the underlying forces that contribute to these associations we performed 2D EXSY <sup>1</sup>H NMR to first determine the orientation of the guest within the host. As Fig. 3 demonstrates the strong binding halogenated adamantanes orient themselves ‘halogen down’, i.e. they display strong carcerisomerism.<sup>26</sup> This was also confirmed in the solid state by the X-ray crystallographic structure of **4** binding iodoadamantane.<sup>7</sup> Furthermore, in addition to providing orientation information the crystal structure also gave insight into one of the driving forces for the complexation of haloalkanes. In the first instance, it was observed that the guest molecule does not reside at the bottom of the hydrophobic pocket. Rather it hovers over a small cavity created as the iodine atom binds only as far down as the benzal hydrogens. In addition, the

**Table 1.** Association constants for various guests binding to molecular basket **4**

Guest	$K_a$ ( $\text{M}^{-1}$ ) in CDCl <sub>3</sub> <sup>a</sup>	$K_a$ ( $\text{M}^{-1}$ ) in toluene- <i>d</i> <sub>8</sub> <sup>a</sup>
Adamantane	– <sup>b</sup>	15
1-Cyanoadamantane	– <sup>b</sup>	36
1-Fluoroadamantane	– <sup>b</sup>	– <sup>b</sup>
1-Chloroadamantane	53	310
1-Bromoadamantane	290	1630
2-Bromoadamantane	78	380
1-Iodoadamantane	670	4390
Bromocamphor	– <sup>b</sup>	150
Bromocycloheptane	5	24
Bromocyclohexane	– <sup>b</sup>	13
Iodocyclohexane	7	35
Bromocyclopentane	– <sup>b</sup>	7
Iodoocyclopentane	– <sup>b</sup>	17
3-Bromopentane	–	– <sup>b</sup>
Iodobenzene	– <sup>b</sup>	– <sup>b</sup>
Bromobenzene	– <sup>b</sup>	– <sup>b</sup>
1-Bromopentane	–	–

At 298 K and 1–5 mM host concentration.

<sup>a</sup> Average for at least three titrations. All associated errors are less than 10%.

<sup>b</sup> NMR signal shifts of the host were apparent, but binding was very weak ( $<5\text{ M}^{-1}$ ).

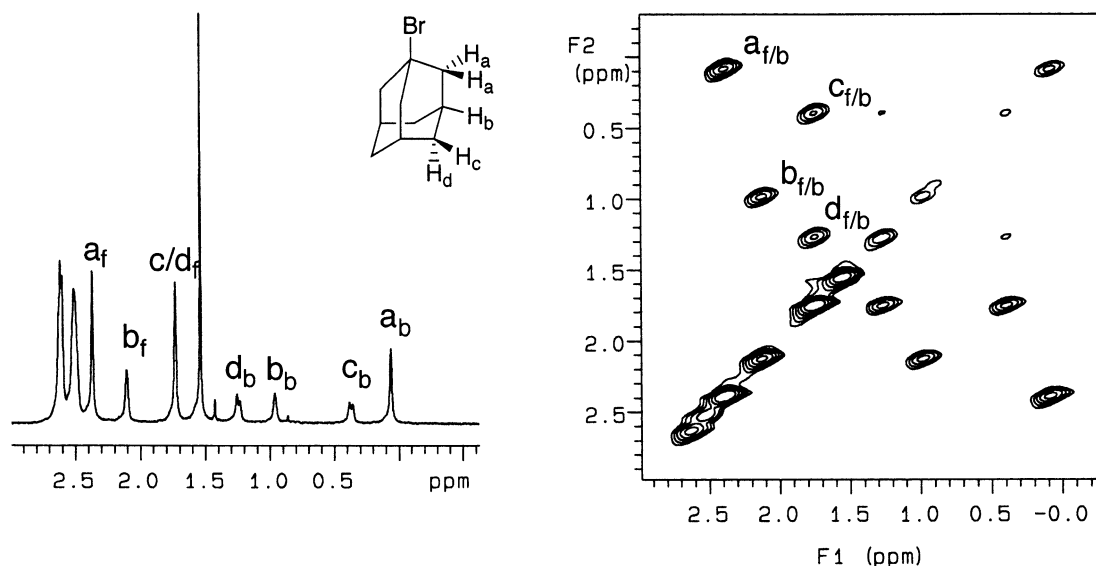


**Figure 3.** Part of a  $^1\text{H}$  NMR spectrum, and the corresponding 2D EXSY spectrum, of 1-bromoadamantane binding to basket **4**. The EXSY spectrum shows the cross-peaks between the guest protons in their free (f) and bound (b) states. Referring to the 1D spectrum, it is apparent that the low-field protons adjacent to the bromine are the most shielded upon complexation, i.e. they are located near the base of the cavity. Note also that because of the  $C_{4v}$  symmetry of the host, the three sets of equivalent protons in the free guest are split into four sets upon complexation.

distance between each benzal hydrogen and the iodine atom of the guest was noted to be less than that the sum of the van der Waals radii for I and H. Finally, the binding process induces a downfield shift in the  $^1\text{H}$  NMR signal of the benzal protons, as is normally observed with the formation of hydrogen bonds. Taken together with the observation that highly polar guests such as cyanoadamantane bind weakly, these results indicate that the formation of multiple  $\text{C}-\text{H}\cdots\text{X}-\text{R}$  hydrogen bonds is a significant driving force for the observed binding.<sup>27</sup>

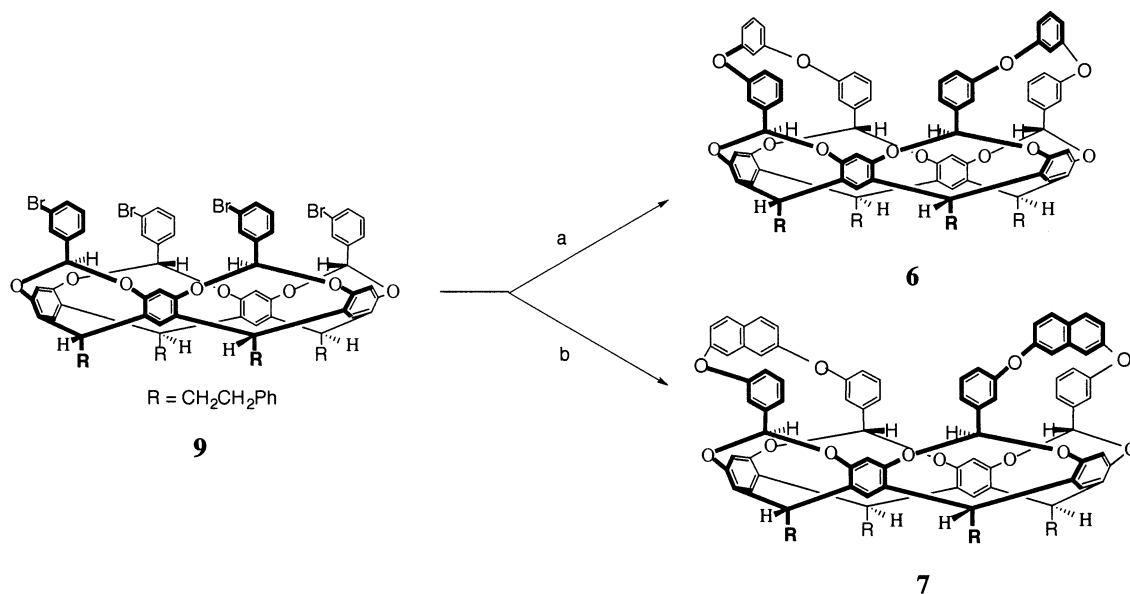
In addition to the importance of having a halogen atom, strong binders should also possess a  $C_n$  rotation axis along the  $\text{C}-\text{X}$  bond. This structural prerequisite allows the guest to bind halogen down yet still freely gyrate around the  $\text{C}-\text{X}$  bond axis without any negative interactions with the walls of the cavity. If the guest does not contain a  $C_n$  axis, then a substantially reduced association constant is observed. For example the binding constant for the  $C_s$  symmetric 2-bromoadamantane is one-fifth that of  $C_{3v}$  1-bromoadamantane (Table 1).

The cavity volume of **4** is estimated to be in the region of  $280 \text{ \AA}^3$ . Thus the binding of haloadamantane guests ranging in size from  $151\text{--}175 \text{ \AA}^3$ ,<sup>28</sup> corresponds to an occupancy factor of ca. 50–60%. However, the relatively rigid nature of the cavity means that the host cannot adjust in size to accommodate larger or smaller guests. Instead guests considerably larger in cross-section than adamantane are expected to be excluded from the cavity, while smaller guests must reside either in a ‘partial vacuum’ or must share the cavity with a solvent molecule.

The examination of caviplex formation with molecules nearly as large or larger than, the cavity of **4** is hampered by availability. There are just not that many readily available molecules that possess quasi-spherical moieties approximately 1 nm in diameter. We first turned to the

ubiquitous  $C_{60}$  that we thought to be too large to fit into the cavity.<sup>29</sup>  $^1\text{H}$  NMR studies demonstrated that this was indeed the case. Moving down in size we next examined 3[(1*R*)-endo]-(+)-bromocamphor (Fig. 2). Possessing one additional oxygen atom than 1-bromoadamantane, this camphor is a slightly bigger guest but has a much smaller association constant in both  $\text{CDCl}_3$  and toluene- $d_8$ . However as expected close examination of the  $^1\text{H}$  NMR of the complex revealed that, as was the case for the haloadamantanes, the bromocamphor binds halogen down. We believe that the slight increase in size is not primarily responsible for this greatly reduced binding. Rather the bulk of this decrease can be attributed to the structure of the guest that results in the carbonyl group impacting the walls of the cavity when it binds halogen down. Hence, thinking in terms of symmetry, it is more appropriate to compare the  $C_1$  camphor binding affinity with that of 2-bromoadamantane.

For guests smaller than bromoadamantane we chose a series of iodo- and bromo-derivatives that would minimally interact with the walls of the cavity. As expected for each guest examined the signal of the reporter benzal hydrogen in the ‘southern hemisphere’ of the cavity moved down-field, indicating the formation of  $\text{C}-\text{H}\cdots\text{X}-\text{R}$  hydrogen bonds as the guest bound in the anticipated manner. All the smaller guests examined were noted to bind much more weakly than the haloadamantanes. For example, the  $C_s$  symmetry series, bromocycloheptane, bromocyclohexane and bromocyclopentane, with molecular volumes of 137, 120, and  $103 \text{ \AA}^3$ , respectively, all bound with association constant less than  $24 \text{ M}^{-1}$ . We attribute this reduced affinity to either the guest residing in a partial vacuum, or to the fact that a solvent molecule must accompany the guest on its journey into the cavity. Unfortunately we were unable to use NMR to identify if the latter scenario was occurring. Any exchange between free and bound solvent is fast on the NMR time-scale and therefore could only be theoretically detected by



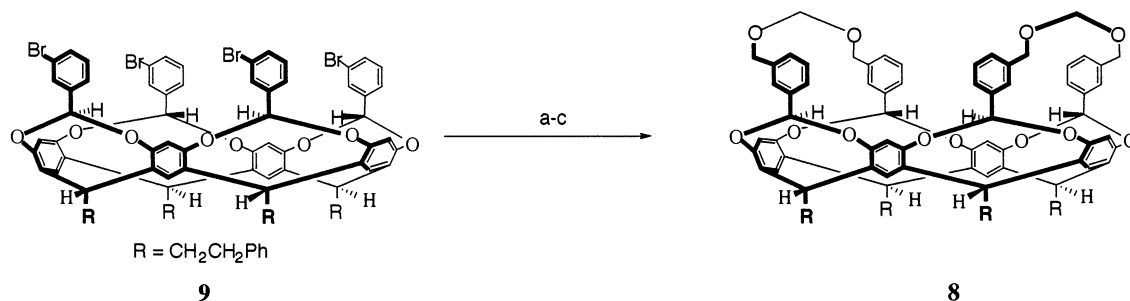
**Scheme 3.** (a) resorcinol, K<sub>2</sub>CO<sub>3</sub>, CuO; (b) 2,7-dihydroxynaphthalene, K<sub>2</sub>CO<sub>3</sub>, CuO.

reference of the residue solvent peak with a (guaranteed) non-binding standard. As expected the related iodides bound more strongly than the bromides, while reducing the preorganization of the guest was detrimental to binding. Thus with respect to the latter, the binding constant of 3-bromopentane (115 Å<sup>3</sup>) is considerably weaker than that of bromocyclopentane, while very little if any binding occurs with 1-bromopentane. Likewise with even smaller guests such as bromo- or iodobenzene (99 and 109 Å<sup>3</sup>, respectively) no significant binding was discernable. Evidently, when the host–guest complex is approximately two-thirds empty space (the occupancy factor of bromocyclopentane is ca. 37%) the association between host and guest is only marginal. To summarize, in non-competitive toluene binding constants are strong at two-thirds occupancy, essentially zero at one-third occupancy, and drop off precipitously in between these two extremes.

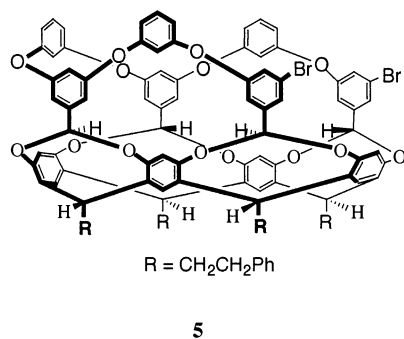
Determining the aforementioned binding constants also gives an insight into the rates of exchange between the free and bound states of the various guests. Several of the cavitplexes studied, in particular those with the largest guests, demonstrated slow guest exchange (at room temperature on the 500 MHz NMR time scale), a feature that is still relatively rare for hosts with open cavities.<sup>15,25,30</sup>

In contrast smaller guests tended to undergo fast exchange. That the adamantanes in particular undergo a slow exchange process is perhaps not too surprising. Either the guest must essentially clear the portal of the host before solvent can rush in and fill the vacuum created by the vacating guest, or a high energy deformation must occur to minimize the volume of the empty cavity.

Host **4** possesses a relatively rigid pocket that undoubtedly contributes significantly to the association constants noted above. To gauge how important this rigidity is, we synthesized the three-quarters basket **5**, and the three half-baskets **6–8** (Scheme 3 and 4). Host **5** was readily isolated in a 20% yield using the same conditions utilized in the synthesis of **4**, but with reduced reaction time. In a similar manner half-baskets **6** and **7** were synthesized from known deep-cavity cavitand **9**<sup>18</sup> (Scheme 3). Thus using the Ullmann ether reaction conditions, the combination of **9** and resorcinol gave hosts **6** in quantitative yield. Similarly reacting **9** with 2,7-dihydroxynaphthalene gave half-basket **7** in 48% yield. Half-basket **8** was also synthesized from **9** in a three step process in which it was first converted to the corresponding tetraaldehyde (Scheme 4). Reduction of this aldehyde with sodium borohydride and alkylation with bromochloromethane gave the desired cavitand.



**Scheme 4.** (a) *n*-BuLi then DMF, then H<sub>3</sub>O<sup>+</sup>; (b) NaBH<sub>4</sub> then H<sub>3</sub>O<sup>+</sup>; (c) *t*-BuOK, BrClCH<sub>2</sub>.



To probe the ability of these molecules to act as hosts we chose our best guest 1-iodoadamantane.<sup>31</sup> CPK models<sup>32</sup> of the three-quarters basket **5** indicate that it is still relatively rigid. However the removal of one aromatic ring has a drastic effect on binding. In deuterio-chloroform an association constant of  $18 \text{ M}^{-1}$ , nearly one-fortieth of that recorded for **4**, was observed. As anticipated, binding was stronger in toluene-*d*<sub>8</sub>, but the recorded value of  $76 \text{ M}^{-1}$  was nearly one-sixtieth of that seen with **4**. In other words, in toluene, removing one ring from the host essentially halved the binding energy from 2.16 to  $1.11 \text{ kcal mol}^{-1}$ . Removing a second ring did likewise. Thus the association constant between host **6** and 1-iodoadamantane was determined to be  $7 \text{ M}^{-1}$  ( $0.5 \text{ kcal mol}^{-1}$ ) in toluene-*d*<sub>8</sub>. No binding was observed in chloroform. These results can be attributed to the loss of preorganization of the cavity that arises when the contiguous chain of eight aromatic rings atop the resorcinarene framework is broken. With this idea in mind we subsequently synthesized related half-basket **7**, and the acetal half-basket **8** to see if a degree of rigidity in the half-basket design could be instilled by changing the atoms connecting one benzal moiety with the next. However both of these derivatives demonstrated even weaker binding than **6**. For example, no binding of 1-iodoadamantane to **7** was observed in either deuterio-chloroform or toluene-*d*<sub>8</sub>, while half-basket **8** fared only slightly better with no binding observed in deuterio-chloroform and an association constant of  $2 \text{ M}^{-1}$  in toluene-*d*<sub>8</sub>. In summary, the binding properties of host **4** are highly dependent on the integral nature of its cavity. Removing the structural elements which bestow the cavity with its non-collapsing nature severely impinge on its affinity for guests.

### 3. Conclusions

As a first step towards the development of reagents that utilize a well-defined hydrophobic pocket for invoking selective catalysis, we have described here the synthesis and binding properties of nano-scale molecular hosts. Computational studies demonstrate an equilibrium between the two (extreme) open and closed conformations of the parent host, but that little of the host exists in the closed form. NMR evidence also supports this latter point. The parent host demonstrates carcerisomerism<sup>26</sup> with strongly bound halogenated guests, and shows good selectivity for guests that are highly complementary with the cavity. In toluene a ‘two-thirds rule’ applied to guests binding into **4**. The cavity of the host–guest complex must be less than two-thirds empty for significant binding to be observed,

with strong (probably optimal binding) seen when the cavity of the complex is approximately two-thirds full. Finally, cavity integrity is essential for binding. Thus even the removal of a small fraction of the cavity wall results in a significant loss or preorganization with attendant loss of strong guest binding. Our current research plans center around the formation of other non-collapsing molecular baskets to garner a firm understanding of the host–guest properties of these types of compounds, and their derivatization to include catalytic machinery within the confines of the hydrophobic pocket. We will report on these findings in due course.

### 4. Insight

There are two facets of molecular cavity synthesis that will figure prominently in future research: cavity size, and the density of information contained within the cavity. The former needs less elaboration than the latter and will be dealt with first by asking the question, ‘how big does a molecular cavity have to be?’ The answer to this question depends on both the purpose of the cavity, as well as the guest target(s). One strong motivator for increasing the cavity size is the development of drug delivery devices. Molecular containers that can carry a number of guests to a specific target and release their cargo at a designed rate are an attractive proposition. Much larger molecular cavities than are currently available will be required for this task. However restricting our thoughts to potential catalytic systems, we should note that unless we are trying to differentiate between two large and structurally similar molecules such as steroids, in most cases it is only necessary to recognize a *part* of *one* molecule. If we set a minimum required host–guest interface of say around  $500 \text{ \AA}^2$ , then the cavity of the host need not be much bigger than that of **4** which already has ca.  $400 \text{ \AA}^2$  of molecular surface to offer the guest. So for many host targets, in terms of cavity size development we are just about there.

Now for the tough part. Consider the physicochemical properties of **4**. What information is contained within its structure that can be transmitted to a guest? Host **4** contains enough information for it to carry out two tasks. It can perform the rudimentary selection of guests, adamantanes over other alkanes, iodides over bromides, over chlorides, etc. and it can induce halogenated guests to adopt a precise orientation within the cavity. Less euphemistically however we can note that it is not near the level of sophistication required to chemically change a guest. Put another way, it is devoid of any transformation information, let alone transformation information that would allow it to bring about catalysis. The development of substrate selective catalysts requires a much higher level of structural complexity. The task at hand therefore is to learn how to pack transformation information into a host cavity, i.e. how to arrange the functional groups that will form an orchestration of non-covalent contacts between host and guest/transition state and engender chemical transformation.<sup>33</sup> Deft synthetic techniques will be required when covalently knitting together such a molecular cavity.

The aforementioned trends point to a general increase in

size of the host whose structure defines the cavity. Thus even if cavity size was not to increase, to introduce more complexity into synthetic cavities will most certainly require a larger 'scaffold' to support the requisite functional groups. This raises the interesting point that three of the most popular supramolecular scaffolds, the cyclodextrins, calixarenes and resorcinarenes, may not be big enough for the job. We have by no means run out of canvas with which to work on these tried and trusted scaffolds, however it may be the case that entirely new canvases, i.e. larger novel macrocycles, will be more suited for catalysts that employ a well defined molecular cavity.<sup>34</sup> Alternatively, advances in self-assembly may be the answer to this dilemma by allowing molecular subunits, each with their own unique surface that will form part of the cavity wall of the assembly product, to be brought permanently together in a specific fashion. Such a modular approach to cavity design will be very powerful strategy for advanced catalyst synthesis.

The continued maturing of supramolecular chemistry will see it begin to meld together several currently disparate fields including classical host–guest chemistry and the development of synthetically useful catalysts. Nature's little reaction chambers provide direct inspiration for this particular amalgamation. However it will only be through diligent design, the development of new synthetic strategies, and/or improved self-assembly methodologies that complex molecular cavity designs capable of catalysis will come to the fore.

## 5. Experimental

### 5.1. General

Synthesis of the requisite starting deep-cavity cavitands **3** and **9** has been reported elsewhere.<sup>18,19</sup> All reagents and guests were purchased from Aldrich Chemical Company. Pyridine was stored over molecular sieves (3A). DMF was stored over molecular sieves and degassed prior to use. Other reagents and guests were used as received. All reactions were run under a nitrogen atmosphere.

Flash chromatography (Silica gel 60 Å, 200–400 mesh; Natland International) was used for product purification. <sup>1</sup>H NMR spectra were recorded on a Varian Unity Inova instrument (500 MHz). MS analysis was performed with a PerSeptive Biosystems Voyager Elite MALDI-TOF instrument. Elemental analysis was performed by Atlantic Microlab. Melting points are uncorrected.

For full details of the binding studies and association constant determinations see Ref. 7.

**5.1.1. Synthesis and characterization of three-quarters basket 5.** To an oven-dried round bottom flask containing 40 mL of pyridine was added 250 mg ( $1.3 \times 10^{-4}$  mol) of octabromide **3**.<sup>18</sup> To this solution was added 220 mg ( $1.5 \times 10^{-3}$  mol) of K<sub>2</sub>CO<sub>3</sub> and 87 mg ( $7.9 \times 10^{-4}$  mol) of resorcinol. Nitrogen was bubbled through the stirring solution for 5 min and 126 mg of CuO ( $1.6 \times 10^{-3}$  mol) was added before the reaction was heated to vigorous reflux

(sand bath) and stirred for 7 days. After cooling, the solvent was removed under reduced pressure to give a crude solid mixture that was suspended in CHCl<sub>3</sub> and loaded onto a short silica plug. Flushing with CHCl<sub>3</sub> and removal of the solvent of the resulting pale yellow solution gave the crude product mixture **4** and **5**. Chromatography (1:1 CHCl<sub>3</sub>/hexane) allowed the isolation of **5** in 21% yield (along with a 38% yield of **4**): mp > 250°C <sup>1</sup>H NMR (400 MHz, CDCl<sub>3</sub>) δ 2.60 (m, 16H), 4.75 (s, 2H), 4.88 (m, 6H), 6.02 (s, 2H), 6.12 (s, 1H), 6.46 (s, 2H), 6.54 (s, 1H), 6.55 (s, 2H), 6.63 (s, 2H), 6.69 (t, 1H, *J* = 2.0 Hz), 6.75 (t, 2H, *J* = 2.0 Hz), 7.03 (m, 4H), 7.13 (m, 8H), 7.24 (m, 20H), 7.41 (m, 2H), 7.54 (t, 2H, *J* = 8.4 Hz), 7.61 (t, 1H, *J* = 8.4 Hz), 7.64 (s, 2H); MS *m/z* (M + Ag<sup>+</sup>)<sup>+</sup> Calculated: 1841.26, Found: 1840.96; Anal. Calcd for C<sub>106</sub>H<sub>76</sub>O<sub>14</sub>Br<sub>2</sub>: C, 73.44; H, 4.42. Found: C, 73.31; H, 4.48.

**5.1.2. Synthesis and characterization of half-basket 6.** To an oven-dried round bottom flask containing 24 mL of pyridine was added 83 mg ( $5.3 \times 10^{-5}$  mol) of tetrabromide **9**.<sup>18</sup> To this stirring solution was added 73.2 mg ( $5.3 \times 10^{-4}$  mol) of K<sub>2</sub>CO<sub>3</sub>, 42 mg of CuO ( $5.3 \times 10^{-4}$  mol) and 33.2 mg ( $3.0 \times 10^{-4}$  mol) of resorcinol. Nitrogen was bubbled through the solution for 5 min before the reaction was heated to vigorous reflux (sand bath) and stirred for 7 days. After cooling, the solvent was removed under reduced pressure to give a crude solid mixture that was suspended in CHCl<sub>3</sub> and loaded onto a short silica plug. Flushing with CHCl<sub>3</sub> and removal of the solvent of the resulting pale yellow solution gave the crude product. Chromatography (1:1 CHCl<sub>3</sub>/hexane), or recrystallization with dichloromethane/acetone, gave the pure product **6** as a colorless solid in quantitative yield: mp > 250°C <sup>1</sup>H NMR (400 MHz, CDCl<sub>3</sub>) δ 2.55 (m, 8H), 2.67 (m, 8H), 4.94 (t, 4H, *J* = 8.0 Hz), 5.09 (s, 4H), 6.28 (s, 2H), 6.48 (s, 4H), 6.58 (s, 2H), 6.85 (dd, 4H, *J* = 8.0, 2.0 Hz), 7.01 (t, 2H, *J* = 2.4 Hz), 7.20 (m, 32H), 7.45 (t, 4H, *J* = 7.8 Hz), 7.52 (d, 4H, *J* = 7.6 Hz); MS *m/z* (M + Ag<sup>+</sup>)<sup>+</sup> Calculated: 1577.56, Found: 1577.63; Anal. Calcd for C<sub>100</sub>H<sub>76</sub>O<sub>12</sub>·H<sub>2</sub>O: C, 80.75; H, 5.25. Found: C, 80.74; H, 5.25.

**5.1.3. Synthesis and characterization of half-basket 7.** To an oven-dried round bottom flask containing 24 mL of pyridine was added 83 mg ( $5.3 \times 10^{-5}$  mol) of tetrabromide **9**.<sup>18</sup> To this stirring solution was added 73.2 mg ( $5.3 \times 10^{-4}$  mol) of K<sub>2</sub>CO<sub>3</sub>, 42 mg of CuO ( $5.3 \times 10^{-4}$  mol) and 42 mg ( $3.0 \times 10^{-4}$  mol) of 2,7-dihydroxynaphthalene. Nitrogen was bubbled through the solution for 5 min before the reaction was heated to vigorous reflux (sand bath) and stirred for 7 days. After cooling, the solvent was removed under reduced pressure to give a crude solid mixture that was suspended in CHCl<sub>3</sub> and loaded onto a short silica plug. Flushing with CHCl<sub>3</sub> and removal of the solvent of the resulting pale yellow solution gave the crude product. Chromatography (1:1 CHCl<sub>3</sub>/hexane), or recrystallization with dichloromethane/acetone, gave the pure product **7** as a colorless solid in 48% yield: mp > 250°C <sup>1</sup>H NMR (400 MHz, CDCl<sub>3</sub>) δ 2.52 (m, 8H), 2.63 (m, 8H), 4.94 (t, 4H, *J* = 8.0 Hz), 5.19 (s, 4H), 6.15 (s, 2H), 6.69 (s, 2H), 7.20 (m, 10H), 7.45 (d, 4H, *J* = 7.6 Hz), 7.52 (t, 4H, *J* = 8.0 Hz), 7.87 (d, 4H, *J* = 8.8 Hz); MS *m/z* (M + Ag<sup>+</sup>)<sup>+</sup> Calculated: 1677.69, Found: 1677.77; Anal. Calcd for C<sub>108</sub>H<sub>80</sub>O<sub>12</sub>·H<sub>2</sub>O: C, 81.72; H, 5.17. Found: C, 81.72; H, 5.51.

## 5.2. Synthesis and characterization of half-basket 8

**5.2.1. Step 1. Synthesis of tetraaldehyde DCC.** To an oven dried flask was added 1.5 g (0.95 mmol) of DCC **9** and 100 mL of dry THF. After dissolution the temperature was reduced to  $-78^{\circ}\text{C}$ . 8 equiv. of *n*-BuLi (7.63 mmol or 8.57 mL of a 0.89 M solution in hexane) were then added drop-wise. After 5 min 20 equiv. of anhydrous DMF (19 mmol or 1.5 mL) dissolved in 10 mL anhydrous THF was added drop-wise and the reaction stirred at  $-78^{\circ}\text{C}$  for 90 min. The reaction was then allowed to warm to  $0^{\circ}\text{C}$  and quenched with 5% HCl until acidic. The mixture was quickly extracted three times with  $\text{CHCl}_3$  and the combined organic layer dried with  $\text{MgSO}_4$ . The solvent was removed under reduced pressure and the product purified by column chromatography using a mobile phase of 2% ethyl acetate/hexane. Removal of the solvent under reduced pressure and drying afforded the desired product as a colorless solid in 64% yield. Mp  $187^{\circ}\text{C}$ .  $^1\text{H NMR}$  ( $\text{CDCl}_3$ )  $\delta$  2.64 (m, 8H), 2.75 (m, 8H), 5.07 (t, 4H,  $J=8.0$  Hz), 5.59 (s, 4H), 6.76 (s, 4H), 7.25 (m, 20H), 7.33 (s, 4H), 7.64 (t, 4H,  $J=7.6$  Hz), 7.93 (dd, 8H,  $J=20$  Hz, 4.4 Hz), 8.20 (s, 4H), 10.07 (s, 4H). MS  $m/z$  ( $\text{M}^+$ ) Calculated: 1369.58, Found: 1370.25. Anal. Calcd for  $\text{C}_{92}\text{H}_{72}\text{O}_{12}$ : C, 80.68; H, 5.30. Found: C, 80.39; H, 5.38.

**5.2.2. Step 2. Synthesis of tetrol DCC.** To an oven dried flask was added 250 mg (0.18 mmol) of the tetraaldehyde DCC, 20 mL dry THF, 4 mL methanol and 4.4 equiv.  $\text{NaBH}_4$  (0.80 mmol, 30.75 mg). The reaction was stirred at room temperature for 1 h. The reaction was then quenched with 5% HCl until acidic, and then quickly partitioned between  $\text{CHCl}_3$  and water. The solvent layers were then separated and the aqueous layer washed with three aliquots of  $\text{CHCl}_3$ . The organic layers were then combined, dried with  $\text{MgSO}_4$ , and the solvent removed under reduced pressure. The product was purified by column chromatography using a mobile phase of 1:1 ethyl acetate/hexane. Removal of the solvent under reduced pressure and drying afforded the desired product as colorless solid in 95% yield. Mp  $190^{\circ}\text{C}$  with decomposition.  $^1\text{H NMR}$  (acetone- $d_6$ )  $\delta$  2.76 (m, 16H), 4.28 (t, 4H,  $J=6.0$  Hz), 4.68 (d, 8H,  $J=6.4$  Hz), 5.06 (s, 4H), 5.61 (s, 4H), 6.95 (s, 4H), 7.26 (m, 20H), 7.41 (m, 8H), 7.62 (m, 4H), 7.78 (s, 4H), 7.87 (s, 4H). MS  $m/z$  ( $\text{M}+\text{Ag}^+$ )<sup>+</sup> Calculated: 1485.51, Found: 1484.62. Anal. Calcd for  $\text{C}_{92}\text{H}_{80}\text{O}_{12}\cdot\text{H}_2\text{O}$ : C, 79.18; H, 5.92. Found: C, 79.31; H, 5.82.

**5.2.3. Step 3. Synthesis of DCC 8.** To an oven-dried round bottom flask was added 50 mg of the tetrol DCC ( $3.6 \times 10^{-5}$  mol) and 30 mL of DMSO. The flask was then placed in a glove box before 5 equiv. of *t*-BuOK ( $1.82 \times 10^{-4}$  mol, 20.4 mg) and 5 equiv of  $\text{CH}_2\text{BrCl}$  ( $1.82 \times 10^{-4}$  mol, 11.8  $\mu\text{L}$ ) were added (with stirring). The reaction was stirred overnight at rt. After this time the solvent was removed under reduced pressure and the crude product partitioned between  $\text{CHCl}_3$  and water. Washing the aqueous layer with a further two aliquots of  $\text{CHCl}_3$ , combining the organic layers and drying with  $\text{MgSO}_4$ , and removal of the solvent under reduced pressure gave the crude product as a white solid. Chromatography (1:2 ethyl acetate/hexane) gave the pure product **8** as a white solid in 24% yield: mp  $210\text{--}215^{\circ}\text{C}$   $^1\text{H NMR}$  (400 MHz,  $\text{CDCl}_3$ )  $\delta$  2.63 (m, 8H),

2.75 (m, 8H), 4.52 (d, 4H,  $J=11.6$  Hz), 4.55 (d, 2H,  $J=5.6$  Hz), 4.66 (d, 2H,  $J=5.6$  Hz), 4.74 (d, 4H,  $J=11.6$  Hz), 5.05 (t, 4H,  $J=7.8$  Hz), 5.35 (s, 4H), 6.59 (s, 2H), 7.08 (s, 2H), 7.24 (m, 28H), 7.30 (s, 2H), 7.40 (m, 4H), 7.43 (s, 2H), 7.60 (s, 4H), 7.76 (d, 4H,  $J=8.0$  Hz); MS  $m/z$  ( $\text{M}+\text{Ag}^+$ )<sup>+</sup> Calculated: 1509.53, Found: 1509.78; Anal. Calcd for  $\text{C}_{94}\text{H}_{80}\text{O}_{12}\cdot\text{H}_2\text{O}$ : C, 79.55 H, 5.78. Found: C, 79.87; H, 5.79.

## Acknowledgements

Special thanks to Pat Lane for her helpful suggestions, and Richard B. Cole of the New Orleans Center for Mass Spectrometry Research. This work was supported by the Donors of the Petroleum Research Fund, administered by the American Chemical Society, the Cancer Association of Greater New Orleans (CAGNO), and the National Science Foundation (CHE-0111133).

## References

1. A partial listing of artificial catalytic systems (both inspired by nature and wholly artificial) follows. For the use of de Novo peptides as catalysts see: (a) Kennan, A. J.; Haridas, V.; Severin, K.; Lee, D. H.; Ghadiri, M. R. *J. Am. Chem. Soc.* **2001**, *123*, 1797–1803. (b) Saghatelian, A.; Yokobayashi, Y.; Soltani, K.; Ghadiri, M. R. *Nature* **2001**, *409*, 797–801. (c) Lee, D. H.; Granja, J. R.; Martinez, J. A.; Severin, K.; Ghadiri, M. R. *Nature* **1996**, *382*, 525–528. For glycoluril derivatives accelerating and catalyzing reactions see: (d) Kang, J.; Rebek, Jr., J. *Nature* **1997**, *385*, 50–52. (e) Kang, J.; Santamaría, J.; Hilmersson, G.; Rebek, Jr., J. *J. Am. Chem. Soc.* **1998**, *120*, 7389–7390. For glycouril based epoxidation catalysts see: (f) Elemans, J. A. A. W.; Bijsterveld, E. J. A.; Rowan, A. E.; Nolte, R. J. M. *Chem. Commun.* **2000**, 2443–2444. For porphyrin based catalysts see: (g) Collman, J. P.; Fu, L. *Acc. Chem. Res.* **1999**, *32*, 455–463. For calixarene based enzyme mimics see: (h) Molenveld, P.; Engbersen, J. F. J.; Reinhoudt, D. N. *Chem. Soc. Rev.* **2000**, *29*, 75–86. (i) Molenveld, P.; Stikvoort, W. M. G.; Kooijman, H.; Spek, A. L.; Engbersen, J. F. J.; Reinhoudt, D. N. *J. Org. Chem.* **1999**, *64*, 3896–3906. (j) Molenveld, P.; Kapsabelis, S.; Engbersen, J. F. J.; Reinhoudt, D. N. *J. Am. Chem. Soc.* **1997**, 2948–2949. For cyclodextrin based enzyme mimics see: (k) Breslow, R. *Acc. Chem. Res.* **1995**, *28*, 146–153. (l) Breslow, R.; Dong, S. D. *Chem. Rev.* **1998**, *98*, 1997–2011. For review of salen based epoxidations and asymmetric ring opening reactions see: (m) Jacobsen, E. N. *Acc. Chem. Res.* **2001**, *33*, 421–431. (n) Jacobsen, E. N. *Transition Metal Catalyzed Oxidations: Asymmetric Epoxidation. Comprehensive Organometallic Chemistry II*; Wilkinson, G., Stone, F. G. A., Abel, E. W., Hegedus, L. S., Eds.; Pergamon: New York, 1995; pp 1097–1135. For asymmetric epoxidation of allylic alcohols/nucleophilic additions/dihydroxylations and hydrogenations see: (o) Berrisford, D. J.; Bolm, C.; Sharpless, K. B. *Angew. Chem., Int. Ed. Engl.* **1995**, *34*, 1059–1070 and references therein. For catalytic asymmetric aminohydroxylations see: (p) Goossen, L. J.; Liu, H.; Dress, K. R.; Sharpless, K. B. *Angew. Chem., Int. Ed. Engl.* **1999**, *38*, 1080–1083. (q) Reddy, K. L.; Sharpless, K. B. *J. Am. Chem. Soc.* **1998**, *120*, 1207–1217. For a review of proline acting as an enantioselective catalyst for aldol condensations see: (r) Gröger,



- H.; Wilken, J. *Angew. Chem., Int. Ed. Engl.* **2001**, *40*, 529–532.
2. Trost, B. M. *Angew. Chem., Int. Ed. Engl.* **1995**, *34*, 259–281.
  3. Gutsche, C. D. *Calixarenes Revisited*; Royal Society of Chemistry: London, 2000.
  4. *Calixarenes in Action*; Mandolini, L., Ungaro, R., Eds.; Imperial College: London, 2000.
  5. Cram, D. J.; Cram, J. M. *Container Molecules and Their Guests*; Royal Society of Chemistry: Cambridge, 1994.
  6. Collet, A. *Tetrahedron* **1987**, *43*, 5725–5759.
  7. Gibb, C. L. D.; Stevens, E. D.; Gibb, B. C. *J. Am. Chem. Soc.* **2001**, *123*, 5849–5850.
  8. Chopra, N.; Sherman, J. C. *Angew. Chem., Int. Ed. Engl.* **1999**, *38*, 1955–1957.
  9. Jasat, A.; Sherman, J. C. *Chem. Rev.* **1999**, *99*, 932–967.
  10. Kim, J.; Jung, I.-S.; Kim, S.-Y.; Lee, E.; Kang, J.-K. K.; Sakamoto, S.; Yamaguchi, K.; Kim, K. *J. Am. Chem. Soc.* **2000**, *122*, 540–541.
  11. Rudkevich, D. M.; Rebek, Jr., J. *Eur. J. Org. Chem.* **1999**, 1991–2005.
  12. Renslo, A. R.; Tucci, F. C.; Rudkevich, D. M.; Rebek, Jr., J. *J. Am. Chem. Soc.* **2000**, *122*, 4573–4582.
  13. Lücking, U.; Tucci, F. C.; Rudkevich, D. M.; Rebek, Jr., J. *J. Am. Chem. Soc.* **2000**, *122*, 8880–8889.
  14. Haino, T.; Rudkevich, D. M.; Rebek, Jr., J. *J. Am. Chem. Soc.* **1999**, *121*, 11253–11254.
  15. Tucci, F. C.; Renslo, A. R.; Rudkevich, D. M.; Rebek, Jr., J. *Angew. Chem., Int. Ed. Engl.* **2000**, *39*, 1076–1079.
  16. Tucci, F. C.; Rudkevich, D. M.; Rebek, Jr., J. *J. Org. Chem.* **1999**, *64*, 4555–4559.
  17. Xi, H.; Gibb, C. L. D.; Stevens, E. D.; Gibb, B. C. *Chem. Commun.* **1998**, 1743–1744.
  18. Xi, H.; Gibb, C. L. D.; Gibb, B. C. *J. Org. Chem.* **1999**, *64*, 9286–9288.
  19. Green, J. O.; Baird, J.-H.; Gibb, B. C. *Org. Lett.* **2000**, *2*, 3845–3848.
  20. Gibb, C. L. D.; Stevens, E. D.; Gibb, B. C. *Chem. Commun.* **2000**, 363–364.
  21. Assuming: (1) that the minor isomer accounts for a measurable fraction of any equilibrium between the major and minor species and; (2) at least a 0.05 ppm shift in a suitable hydrogen atom occurs; a coalescence temperature ( $T_c$ ) of  $-90^\circ\text{C}$  would give a rate constant ( $k_c=2.22\Delta\nu$ ) of  $55.5\text{ s}^{-1}$ . Thus using the Eyring equation ( $\Delta G^\ddagger=4.58T_c[10.32+\log(T_c/k_c)]$ ), for the scenario where the barrier to flipping is low, the free energy of activation ( $\Delta G^\ddagger$ ) for the flipping process must be of less than ca.  $9\text{ kcal mol}^{-1}$ . See: *Basic One- and Two-Dimensional NMR Spectroscopy*; Friebolin, H., Ed.; 3rd ed, Wiley-VCH: Weinheim, 1998.
  22. *Chem 3D*, Pro version 3.5.1; Cambridge Soft Corporation 02139: Cambridge Massachusetts, USA.
  23. Frisch, M. J.; Trucks, G. W.; Schlegel, H. B.; Scuseria, G. E.; Robb, M. A.; Cheeseman, J. R.; Zakrzewski, V. G.; Montgomery, J. A.; Stratmann, R. E.; Burant, J. C.; Dapprich, S.; Millam, J. M.; Daniels, A. D.; Kudin, K. N.; Strain, M. C.; Farkas, O.; Tomasi, J.; Barone, V.; Cossi, M.; Cammi, R.; Mennucci, B.; Pomelli, C.; Adamo, C.; Clifford, S.; Ochterski, J.; Petersson, G.; Aayala, P. Y.; Cui, Q.; Morokuma, K.; Malick, D. K.; Rubuck, A. D.; Raghavachari, K.; Foresman, J. B.; Cioslowski, J.; Ortiz, J. V.; Stefanov, B. B.; Lui, G.; Liashenko, A.; Piskorz, P.; Komaromi, I.; Gomperts, R.; Martin, R. L.; Fox, D. J.; Keith, T.; Al-Laham, M. A.; Peng, C. Y.; Nanayakkara, A.; Gonzalez, C.; Challacombe, M.; Gill, P. M. W.; Johnson, B. G.; Chen, W.; Wong, M. W.; Andres, J. L.; Head-Gordon, M.; Replogle, E. S.; Pople, J. A.; *Gaussian 98*, Revision A.5; Gaussian, Inc: Pittsburgh, PA, 1998.
  24. The SVWN procedure invokes the local spin density approximation and involves Slater exchange: Slater, J. C. *The Self-Consistent-Field for Molecules and Solids; Quantum Theory of Molecules and Solids*, Vol. 4; McGraw-Hill: New York, 1974. The Vosko–Wilk–Nusair correlation function: Vosko, S. H.; Wilk, L.; Nusair, M. *Can. J. Phys.* **1980**, *58*, 1200.
  25. For topologically related hosts that demonstrate dynamic lowering and raising of their cavity walls see: (a) Saito, S.; Nuckolls, C.; Rebek, Jr., J. *J. Am. Chem. Soc.* **2000**, *122*, 9628–9630. (b) Rudkevich, D. M.; Hilmersson, G.; Rebek, Jr., J. *J. Am. Chem. Soc.* **1997**, *119*, 9911–9912. (c) Rudkevich, D. M.; Hilmersson, G.; Rebek, Jr., J. *J. Am. Chem. Soc.* **1998**, *120*, 12216–12217. (d) Renslo, A. R.; Rudkevich, D. M.; Rebek, Jr., J. *J. Am. Chem. Soc.* **1999**, *121*, 7459–7460. (e) Ma, S.; Rudkevich, D. M.; Rebek, Jr., J. *Angew. Chem., Int. Ed. Engl.* **1999**, *38*, 2600–2602. (f) For additional examples see Refs. 11–16.
  26. Timmerman, P.; Verboom, W.; van Veggel, F. C. J. M.; van Duynhoven, J. P. M.; Reinhoudt, D. N. *Angew. Chem., Int. Ed. Engl.* **1994**, *33*, 2345–2348.
  27. We use the term hydrogen bonds to refer to the interaction between host and guest that occurs via the four benzal hydrogens. Out of the various components that can be conceived to contribute to a hydrogen bond (including: classical electrostatic interactions such as monopole–monopole and dipole–dipole interactions; and polarization effects such as exchange repulsion, charge transfer and dispersion interactions, we anticipate that dispersion forces are the major contributor to these hydrogen bonds. Thus the iodine atom, which is large enough to form four hydrogen bonds and is highly polarizable, forms the strongest interactions with the host. As the respective halogen atoms decrease in size they can simultaneously interact with fewer benzal hydrogens and are also less polarizable. Consequently binding decreases from R–I guests through those with R–F functionality. It may be suggested that the term, dispersion forces be used instead of C–H $\cdots$ X–R hydrogen bonds, however the former term is usually used for diffuse and unfocused interactions, rather than the highly focused and directional interactions apparent in this host–guest system. See: Jeffrey, G. A. *An Introduction to Hydrogen Bonding*; Oxford University Press: New York, 1997 and references therein.
  28. Bondi, A. *J. Phys. Chem.* **1964**, *68*, 441–451.
  29. Ruelle, P.; Farina-Cuendet, A.; Kesselring, U. *Chem. Commun.* **1995**, 1161.
  30. Kobayashi, K.; Asakawa, Y.; Kikuchi, Y.; Toi, H.; Aoyama, Y. *J. Am. Chem. Soc.* **1993**, *115*, 2648–2654.
  31. For a full description of the experimental techniques used for the determination of the association constants, see Ref. 7. As for the tabulated results, the following association constants are the average of at least three titrations. Associated errors are  $\pm 10\%$ .
  32. Koltun, W. L. *Biopolymers* **1965**, *3*, 665–679.
  33. For recent advances in this direction see: (a) Renslo, A. R.; Rebek, Jr., J. *Angew. Chem., Int. Ed. Engl.* **2000**, *39*, 3281–3283. (b) Wash, P. L.; Renslo, A. R.; Rebek, Jr., J. *Angew. Chem., Int. Ed. Engl.* **2001**, *40*, 1221–1222.
  34. For one interesting possibility see: Naumann, C.; Roman, E.; Peinador, C.; Ren, T.; Patrick, B. O.; Kaifer, A. E.; Sherman, J. C. *Chem. Eur. J.* **2001**, *7*, 1637–1645.